Materials Express

2158-5849/2016/6/191/007
doi:10.1166/mex.2016.1292
www.aspbs.com/mex

Communication

Novel volatile organic compound (VOC) sensor based on Ag-decorated porous single-crystalline ZnO nanosheets

Yufeng Sun[1,2], Sheng Ge[1,2], Huanhuan Huang[3], Hanxiong Zheng[1,2], Zhen Jin[2,*], Jianhua Shan[4], Cuiping Gu[3,*], Xingjiu Huang[1,2], and Fanli Meng[2,*]

[1]*Department of Mechanical and Automotive Engineering, Anhui Polytechnic University, Wuhu 241000, China*
[2]*Nanomaterials and Environment Detection Laboratory, Institute of Intelligent Machines, Chinese Academy of Sciences, Hefei 230031, China*
[3]*College of Chemistry and Materials Science, Center for Nano Science and Technology, Anhui Normal University, Wuhu 241000, China*
[4]*School of Mechanical Engineering, Anhui University of Technology, Maanshan 243002, China*

ABSTRACT

To develop efficient and convenient sensing technology for volatile organic compound (VOCs) detection in residential buildings and process control in industries becomes necessary for human health. Various ZnO nanostructures have been employed in VOC detection for their good performance. Among those nanostructures, porous single-crystalline (PSC) ZnO nanosheets not only exhibited highly-sensitive performance but also possessed significantly long-term stability. However, the sensitivity might be further improved by modification noble metal elements. In present work, Ag nanoparticles have been decorated onto the PSC ZnO nanosheets by a sunlight induced solvent reduction method. The as-prepared products have been characterized by SEM, TEM, HRTEM and EDS. By combining the advantages of structure and modification, the sensitivity of the Ag-decorated PSC ZnO nanosheets is 8.8 times higher than that of the bare one. The single-crystalline structure exhibited low electric noise which may lower the detection limit of the sensor.

Keywords: Volatile Organic Compound (VOC), Ag-Decorated, Porous, ZnO Nanosheet.

1. INTRODUCTION

Volatile organic compounds (VOCs) are those organic chemicals having a high vapor pressure at room temperature.[1] Some VOCs are common indoor air pollutions (e.g., formaldehyde) and some are important products in industry (e.g., acetone and furan). Therefore, to develop efficient and convenient sensing technology for VOC detection in residential buildings and process control in industries becomes necessary for human health.

Metal oxide gas sensors (e.g., ZnO, SnO_2, In_2O_3, etc) have been widely used in portable gas detection systems because of their good performance including low cost, easy production, compact size and simple measuring electronics.[2–7] However, their gas sensing properties are significantly influenced by morphology and structure, so that it is difficult for bulk material or dense film based gas sensors to achieve highly sensitive properties. Nanostructured metal oxide semiconductors are a great developing direction to improve gas sensing properties in sensitivity, selectivity and response speed.[8–12] For example, Guan et al. synthesized Zn-doped SnO_2 hierarchical architectures composed of many two dimensional nanosheets, which

*Authors to whom correspondence should be addressed.
Emails: zjin@iim.ac.cn, cpgu2008@mail.ahnu.edu.cn, flmeng@iim.ac.cn

showed excellent selectivity toward ethanol.[13] Li et al. prepared meso-macroporous SnO_2 structure to improve the sensitivity and response speed.[14] Fang et al. fabricated coralloid hierarchical SnO_2 nanostructures by a solvothermal route, which exhibited high sensitivity, short recovery time, good reproducibility and linear dependence relation to benzaldehyde and acetone.[15]

In the past decades, ZnO has been widely investigated because of its excellent electronic and photonic properties.[16, 17] Various ZnO nanostructures with different morphologies, such as nanowires,[18, 19] nanorods,[20–22] nanosheets[23] and nanospheres[24] have been developed to improve the gas sensing performance. Gu et al. synthesized porous flower-like ZnO nanostructures which exhibited good response and reversibility to VOCs.[25] Alenezi et al. prepared ZnO hierarchical structures with high surface-to-volume ratios and an increased proportion of exposed active planes, which displayed significantly improved sensitivity and fast response to acetone.[26] Compared to those nanostructures, porous single-crystalline (PSC) ZnO nanosheets not only exhibited highly-sensitive performance but also possessed significantly long-term stability.[27]

Besides of morphology and structure for sensing materials, modification with rare-earth and noble metal elements is also a common and effective method to improve sensing properties.[28] Up to now, significant efforts have been made to improve the sensitivity and selectivity to volatile organic compound by doping Ag element in ZnO nanomaterials.[29–33] By combining the advantages of structure and modification, Ag nanoparticles here have been decorated onto the PSC ZnO nanosheets by a sunlight induced solvent reduction method, which exhibited 8.8 times higher response than the bare one. The single-crystalline structure exhibited low electric noise which may lower the detection limit of the sensor.

2. EXPERIMENTAL DETAILS

2.1. Materials Characterization

All reagents were commercially available from Sinopharm Chemical Reagent Co., Ltd. (China) with analytical grade and were used without further purification.

The as-prepared samples were characterized by field-emission scanning electron microscopy (FE-SEM, FEI Sirion-200), high resolution transmission electron microscopy (HRTEM, JEOL JEM-2011) and energy dispersive spectroscopy (EDS, Oxford INCA X-Max 50).

2.2. Preparation of PSC ZnO Nanosheets

The PSC ZnO nanosheets were firstly prepared by a one-pot wet-chemical method followed by an annealing treatment.[34] Typically, 3.0 g of urea and 1.0 g of zinc acetate were dissolved into deionized water (40 mL) and then stirred for 30 min. The solution was sealed in a conical flask and then placed in an oven at 100 °C for 6 h. When it naturally cooled down, the precipitate was centrifuged, washed with deionized water and dried at 60 °C in sequence. Then, the precursors were annealed at 300 °C for 2 h in air and the PSC ZnO nanosheets were obtained. Finally, the PSC ZnO nanosheets were modified by Ag particles using sunlight induced solvent reduction method. Typically, 30 mg of $AgNO_3$ was dissolved into 30 mL of ethanol and then 20 mg of the prepared PSC ZnO nanosheets were added. After stirring for 30 min under sunlight irradiation, the Ag-decorated PSC ZnO nanosheets were obtained.

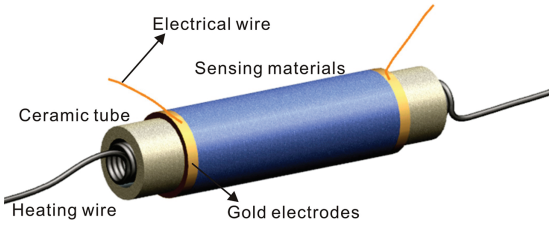

Fig. 1. The structure of the gas sensor.

2.3. Fabrication of Gas Sensor

The structure of the gas sensor as shown in Figure 1 was showed in our previous work.[35, 36] Typically, a pair of gold electrodes was firstly fabricated onto a ceramic tube by thick film technology. And then two pairs of electrical wires were connected to them. A piece of nichrome wire (~30 Ω) was placed in the interior of the ceramic tube as heating wire. To fabricate a gas sensor, the as-prepared samples of the Ag-decorated PSC ZnO nanosheets were directly coated on the surface of the ceramic tube and then dried in an infrared drying oven followed by an annealing treatment in a muffle furnace at 350 °C for 2 h in air.

3. RESULTS AND DISCUSSION

3.1. Materials Characterization

The PSC ZnO nanosheets were firstly synthesized by a one-pot wet-chemical method followed by an annealing treatment. The formation process of the PSC ZnO nanosheets may be explained by the following sequence of reactions:

$$CO(NH_2)_2 + 3H_2O \rightarrow CO_2 \uparrow + 2NH_4OH \quad (1)$$

$$NH_4OH \rightarrow NH_4^+ + OH^- \quad (2)$$

$$4Zn^{2+} + CO_2 + 6OH^- + 2H_2O \rightarrow Zn_4CO_3(OH)_6 \cdot H_2O + 2H^+ \quad (3)$$

$$Zn_4CO_3(OH)_6 \cdot H_2O \rightarrow 4ZnO + CO_2 \uparrow + 4H_2O \uparrow \quad (4)$$

Then, the Ag particles were modified onto the PSC ZnO nanosheets by a sunlight induced solvent reduction method, which is helpful for remaining the morphology of the PSC ZnO nanosheets.

The microstructures of the as-prepared PSC ZnO nanosheets were firstly characterized by TEM and HRTEM

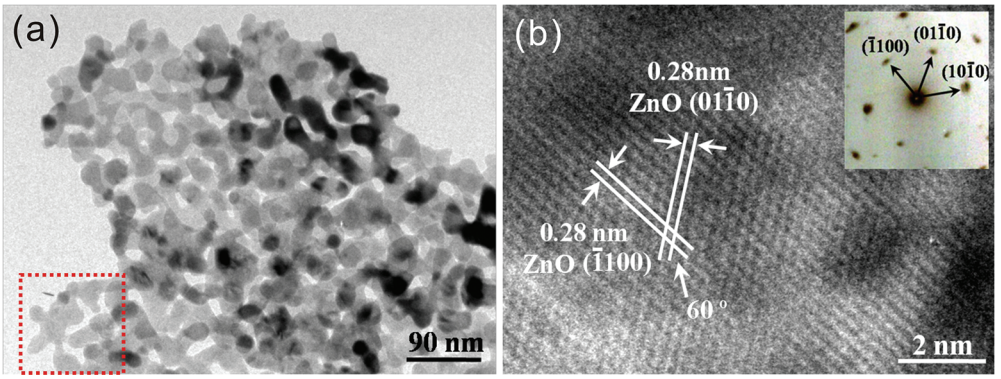

Fig. 2. (a) TEM image of the PSC ZnO nanosheets. (b) Lattice-resolved HRTEM image of the selected area in (a) and the corresponding SAED pattern.

to reveal specific characteristics. Figure 2(a) exhibits the typical TEM image of an individual nanosheet, from which it can be clearly seen that a large number of mesopores with irregular size uniformly covers the nanosheet. The lattice-resolved HRTEM image (Fig. 2(b)) exhibits that many clear and coherent lattice fringes with 0.28 nm of lattice spacing cover the whole nanosheet, which is indexed to the ($\bar{1}$100) planes of the hexagonal phase of ZnO. The inset in Figure 2(b) presents the corresponding SAED, from which it can be seen that the diffraction pattern consists of well ordered dots, indicating the single crystallinity of the porous nanoplates. The crystalline planes ($\bar{1}$100), (01$\bar{1}$0) and (10$\bar{1}$0) of wurtzite ZnO can be indexed from the SAED pattern. Both the SAED pattern and HRTEM image indicate that these nanosheets are actually porous single crystals with high quality.

The morphologies of the as-prepared Ag-decorated PSC ZnO nanosheets were then characterized by SEM and the result are shown in Figure 3. There are numerous randomly placed nanosheets with sub-micrometer in width and a few micrometers in length. Many mesopores can also be clearly observed in each nanosheet, which is well coincident with the TEM characterization of the PSC ZnO nanosheet. Although the Ag particles were too small to be observed from the surfaces of the nanosheets, TEM analysis was employed to further observe the size of Ag nanoparticles as shown in Figure 4. It can be seen that the size of the Ag nanoparticle is about 6–15 nm. EDS spectrum is shown in Figure 5, from which a weak Ag peak can be observed. The amount of Ag is calculated to be 1 wt%.

3.2. Operating Temperature

The gas sensing performance of the Ag-decorated PSC ZnO nanosheets was firstly measured by a homemade gas sensing measurement apparatus as shown in our previous work.[35, 36] A sensor was placed in a closed test chamber (1000 mL) equipped with appropriate inlets and outlets for gas flow. A Keithley 6487 source/measure unit was used to record the change of current as well as to provide a power source. When the source/measure unit working, a constant bias voltage was applied onto the electrodes between the sensing films and then the current flowing through it was measured and recorded. The source/measure unit was usually operated under the condition that bias voltage

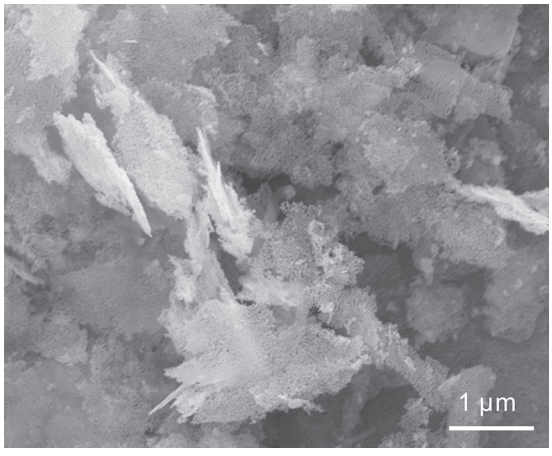

Fig. 3. SEM image of the Ag-decorated PSC ZnO nanosheets.

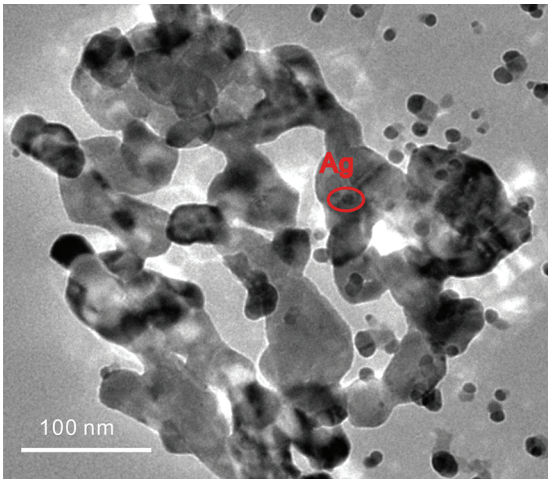

Fig. 4. TEM image of the Ag-decorated PSC ZnO nanosheet.

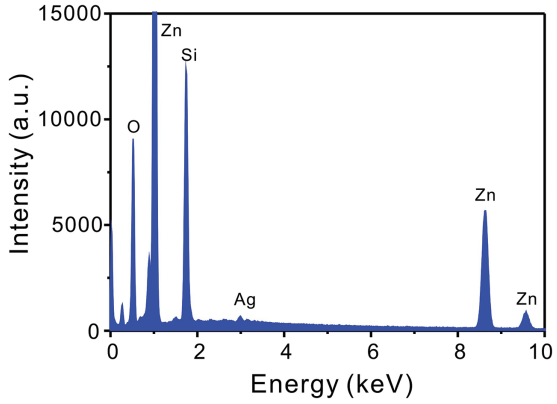

Fig. 5. EDS spectrum of the Ag-decorated PSC ZnO nanosheets.

is 1 V and the aperture time of acquiring data is 0.5 s. Typically, a gas sensing measurement was performed as follows: the saturated organic vapors under a standard atmospheric pressure were introduced into the test chamber by a microsyringe and then the source/measure unit acquire the current change and record it. Once a gas sensing measurement was over, the target gases in the testing chamber were released by inputting fresh air.

The response of the sensor is defined as

$$\text{Response} = \frac{I_g - I_a}{I_a} \times 100\% \quad (5)$$

Here, I_a and I_g are the electric current of the sensor in air and target gas, respectively.

Generally, operating temperatures highly affect the sensing performance of metal oxide gas sensors. Therefore, the responses of the Ag-decorated PSC ZnO nanosheet to 100 ppm of formaldehyde at different operating temperatures were firstly investigated as shown in Figure 6. From the temperature dependence studies, it can be clearly seen that the responses present a peak at 300 °C with

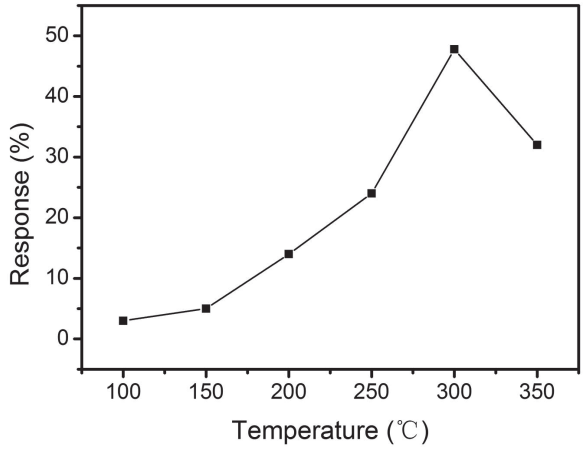

Fig. 6. Plots of the response versus working temperature of the Ag-decorated PSC ZnO nanosheets to 100 ppm of formaldehyde.

increasing operating temperature. Therefore, the following tests of the sensors based on the Ag-decorated PSC ZnO nanosheets were all adopted at 300 °C. On the surface of the sensor, target gas can react with the adsorbed oxygen species to different degrees according to the activity of the adsorbed oxygen species. In previous reports,[37] there are two different oxygen species on the surface under different temperatures, i.e., molecular (O_2^-) and atomic (O^-, O^{2-}) oxygen species. Molecular form usually exists below 150 °C, while atomic species dominate at higher temperature. Therefore, the sensor worked mostly depending on atomic species at 300 °C.

3.3. Comparison of Ag-Decorated PSC ZnO Nanosheets with Bare PSC ZnO Nanosheets

The gas sensing performance of the Ag-decorated PSC ZnO nanosheets to furan, a kind of persistent organic pollutants (POP) stimulant, was investigated coupling with a gas chromatography column by comparing with the bare PSC ZnO nanosheets. A sample injection port and a gas chromatography column were placed in front of a metal oxide sensor to separate furan from the mixture,[38, 39] which may gasify the target molecules and separate them with solvents. This test method can be used to detect most of the POPs of furans. N_2 controlled by a carrier gas controller was used as carrier gas to flow through a SE-54

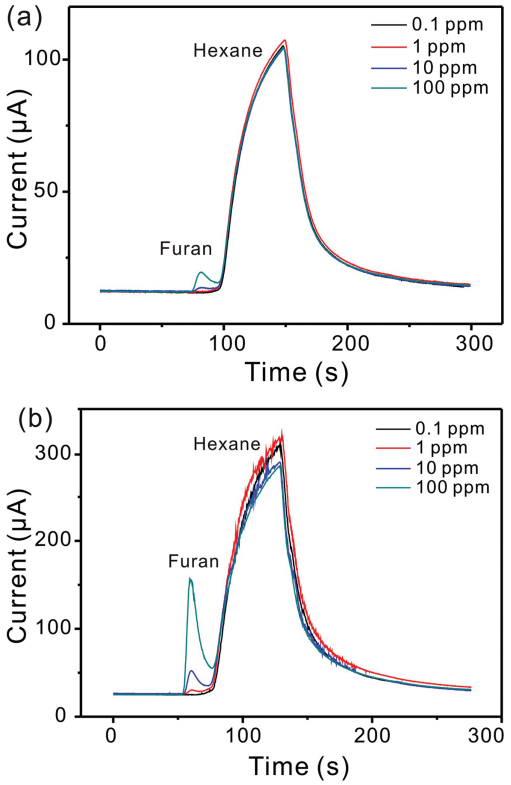

Fig. 7. Real-time response curves of (a) the bare PSC ZnO nanosheets and (b) the Ag-decorated PSC ZnO nanosheets to the mixture of hexane and furan working at 300 °C.

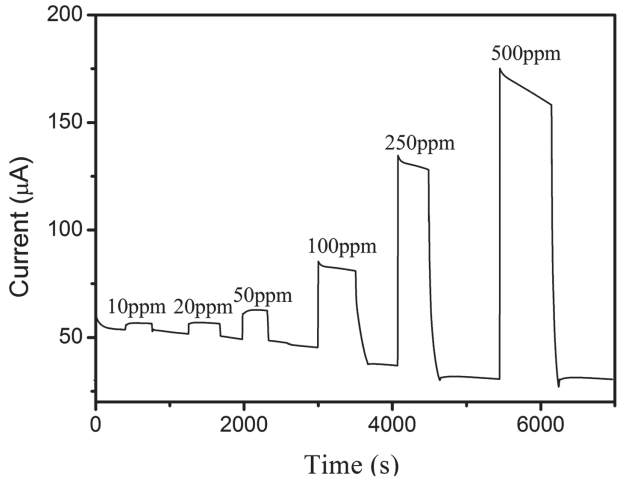

Fig. 8. Real-time responses of the Ag-decorated PSC ZnO nanosheets to different concentrations of formaldehyde working at 300 °C.

capillary column (30 m, 0.25 mm i.d., 1.0 μm film thickness) placed in a temperature-controlled column oven. Air was mixed in the outlet of the chromatography column. A mass flow controller (MFC, Sevenstar CS200) were used to control the flow rate of gases. The pressure of the carrier gas controller was 0.2 MPa. The temperature of the injection port was set to 100 °C. The mixture sample of furan and n-hexane was once injected by 0.5 μL and the temperature of the column oven was set to 50 °C. The real-time response curves of the bare and the Ag-decorated PSC ZnO nanosheets to different concentrations of furan mixture are shown in Figure 7, respectively. It can be seen that the responses of the Ag-decorated PSC ZnO nanosheets are much higher than that of the bare one. The response to 100 ppm of furan is 8.8 times higher response than the bare one.

The modification of Ag nanoparticle played an important role to improve the sensitivity of the PSC ZnO nanosheets because it possesses high catalytic activity and consequently increases the reaction activity of the space-charge layers. According to previous report,[33] AgO exists at the initial state of the sensing material. When it is heated, AgO will transform to Ag. In air, the oxygen molecules react preferentially with the Ag nanoparticles forming oxygen anions and then spill over to the ZnO matrix. The target gases might be adsorbed onto the surface of the Ag nanoparticles and then migrate to the surface of ZnO nanosheets to react with surface oxygen species thereby increasing the surface conductivity. Therefore, the Ag-decorated PSC ZnO nanosheets are more sensitive than the bare one.

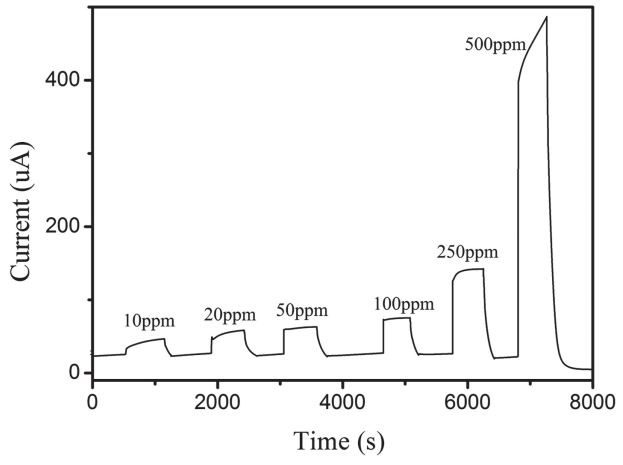

Fig. 9. Real-time responses of the Ag-decorated PSC ZnO nanosheets to different concentrations of acetone working at 300 °C.

3.4. Response of Ag-Decorated PSC ZnO Nanosheets to VOCs

To quantitatively investigate the gas sensing properties of the Ag-decorated PSC ZnO nanosheets to VOCs, the homemade gas sensing measurement apparatus was used and different concentrations of VOCs (formaldehyde and acetone) were also measured. Figure 8 shows the real-time responses of the Ag-decorated PSC ZnO nanosheets to different concentrations of formaldehyde. The responses increase linearly with the concentration increasing from 10 to 500 ppm. The response time is defined as the time when the change of current reaches 90% of the balanced current on exposure to a target gas. Similarly, the recovery

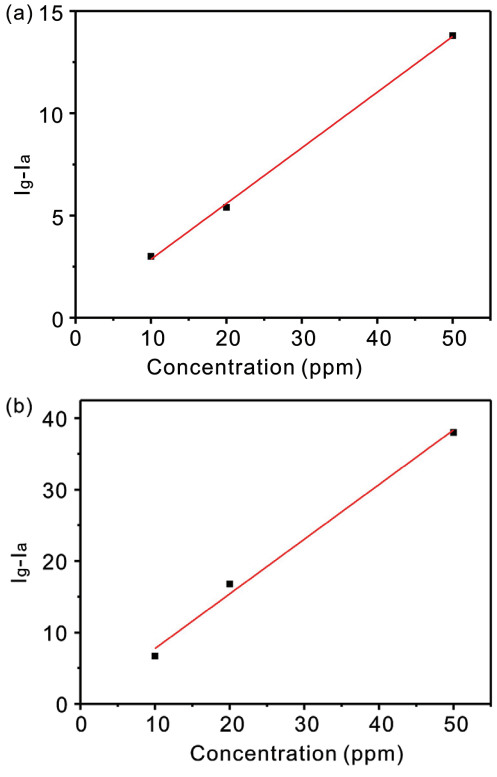

Fig. 10. Plots of the (I_g–I_a) versus concentration for (a) formaldehyde and (b) acetone obtained from Figures 8 and 9.

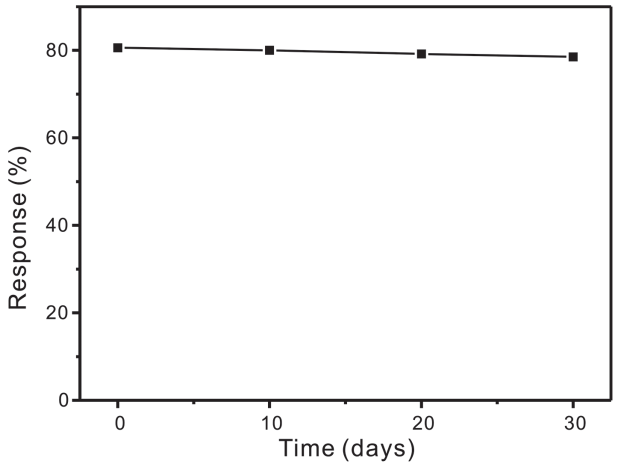

Fig. 11. Stability of the Ag-decorated PSC ZnO nanosheets to 100 ppm of formaldehyde at 300 °C.

time is defined as the time reached a 90% reversal of the current. The response of the sensor to 500 ppm of formaldehyde is 409%, while the response and recovery time is 5 s and 30 s, respectively. From Figure 9, it can be seen that the response to acetone is much higher to formaldehyde. But the response and recovery times to acetone are longer than to formaldehyde. The response of the sensor to 500 ppm of acetone is 1736%, while the response and recovery time is 7 s and 100 s, respectively. From the response curves, it can be observed that the Ag-decorated PSC ZnO nanosheets possess low electric noise (~56 nA) and high signal-to-noise ratio (S/N), which may be attributed to the single-crystalline structure. For well linear relationship, the responses of the lowest three concentrations are used to calculate the detection limits as shown in Figure 10. The detection limits are calculated to be 0.18 and 0.1 ppm (using S/N = 3) for formaldehyde and acetone, respectively. The single-crystalline structure is favorable for electronic transportation and may reduce electron scattering. Therefore, the Ag-decorated PSC ZnO nanosheets possess low electric noise.

3.5. Stability of Ag-Decorated PSC ZnO Nanosheets

For practical applications, the gas sensing stability of the sensor device is a very important parameter. Figure 11 shows the long-term stability of the Ag-decorated PSC ZnO nanosheets to 100 ppm of formaldehyde at 300 °C, from which it can be seen that the response only decrease a little a month later. Therefore, the Ag-decorated PSC ZnO nanosheets exhibited very good stability which was suitable for the practical application.

4. CONCLUSION

Sunlight induced solvent reduction method has been used to modify Ag nanoparticles onto the surface of the PSC ZnO nanosheet which were prepared by one-pot wet-chemical method followed by an annealing treatment. The SEM, TEM and SAED results confirmed the porous and single-crystalline structure of the ZnO nanosheets. The EDS measurement ensures that Ag nanoparticles have been modified onto the PSC ZnO nanosheets. The sensing detection results exhibited that the response of the Ag-decorated PSC ZnO nanosheets were 8.8 times higher than that of the bare one and the detection limit reached 0.1 ppm, which demonstrates the potential application of the Ag-decorated PSC ZnO nanosheets for fabricating high sensitive gas sensors.

Acknowledgments: We appreciate the financial support of the National Natural Science Foundation of China (61374017, 61174012, 61203212 and 51405001) and the Key Technologies R&D Program of Anhui Province (1501021005).

References and Notes

1. B. Li, J. F. Liu, G. L. Shi, and J. H. Liu; A research on detection and identification of volatile organic compounds utilizing cataluminescence-based sensor array; *Sens. Actuat. B* 177, 1167 **(2013)**.
2. N. Yamazoe, G. Sakai, and K. Shimanoe; Oxide semiconductor gas sensors; *Catal. Surv. Asia* 7, 63 **(2003)**.
3. E. Comini; Metal oxide nano-crystals for gas sensing; *Anal. Chim. Acta* 568, 28 **(2006)**.
4. F. L. Meng, N. N. Hou, Z. Jin, B. Sun, W. Q. Li, X. H. Xiao, C. Wang, M. Q. Li, and J. H. Liu; Sub-ppb detection of acetone using Au-modified flower-like hierarchical ZnO structures; *Sens. Actuat. B* 219, 209 **(2015)**.
5. Y. F. Sun, X. J. Huang, F. L. Meng, and J. H. Liu; Study of influencing factors of dynamic measurements based on SnO_2 gas sensor; *Sensors* 4, 95 **(2004)**.
6. H. Wu, C. Xu, J. Xu, L. F. Lu, Z. Y. Fan, X. Y. Chen, Y. Song, and D. D. Li; Enhanced supercapacitance in anodic TiO_2 nanotube films by hydrogen plasma treatment; *Nanotechnology* 24, 455401 **(2013)**.
7. H. Wu, D. D. Li, X. F. Zhu, C. Y. Yang, D. F. Liu, X. Y. Chen, Y. Song, and L. F. Lu; High-performance and renewable supercapacitors based on TiO_2 nanotube array electrodes treated by an electrochemical doping approach; *Electrochim. Acta* 116, 129 **(2014)**.
8. M. E. Franke, T. J. Koplin, and U. Simon; Metal and metal oxide nanoparticles in chemiresistors: Does the nanoscale matter?; *Small* 2, 36 **(2006)**.
9. M. Tiemann; Porous metal oxides as gas sensors; *Chem.-Eur. J.* 13, 8376 **(2007)**.
10. A. Tricoli, M. Righettoni, and A. Teleki; Semiconductor gas sensors: Dry synthesis and application; *Angew. Chem. Int. Edit.* 49, 7632 **(2010)**.
11. J. H. Lee; Gas sensors using hierarchical and hollow oxide nanostructures: Overview; *Sens. Actuat. B* 140, 319 **(2009)**.
12. C. Xu, Y. Song, L. F. Lu, C. W. Cheng, D. F. Liu, X. H. Fang, X. Y. Chen, X. F. Zhu, and D. D. Li; Electrochemically hydrogenated TiO_2 nanotubes with improved photoelectrochemical water splitting performance; *Nanoscale Res. Lett.* 8, 391 **(2013)**.
13. Y. Guan, D. W. Wang, X. Zhou, P. Sun, H. Y. Wang, J. Ma, and G. Y. Lu; Hydrothermal preparation and gas sensing properties of Zn-doped SnO_2 hierarchical architectures; *Sens. Actuat. B* 191, 45 **(2014)**.
14. H. H. Li, F. L. Meng, J. Y. Liu, Y. F. Sun, Z. Jin, L. T. Kong, Y. J. Hu, and J. H. Liu; Synthesis and gas sensing properties of hierarchical meso-macroporous SnO_2 for detection of indoor air pollutants; *Sens. Actuat. B* 166, 519 **(2012)**.

Communication

15. C. H. Fang, S. Z. Wang, Q. Wang, J. Liu, and B. Y. Geng; Coralloid SnO_2 with hierarchical structure and their application as recoverable gas sensors for the detection of benzaldehyde/acetone; *Mater. Chem. Phys.* 122, 30 **(2010)**.
16. M. L. Yin, M. D. Liu, and S. Z. Liu; Diameter regulated ZnO nanorod synthesis and its application in gas sensor optimization; *J. Alloy Compd.* 586, 436 **(2014)**.
17. H. Y. Song, H. Yang, and X. C. Ma; A comparative study of porous ZnO nanostructures synthesized from different zinc salts as gas sensor materials; *J. Alloy Compd.* 578, 272 **(2013)**.
18. L. W. Wang, S. R. Wang, M. J. Xu, X. J. Hu, H. X. Zhang, Y. S. Wang, and W. P. Huang; A Au-functionalized ZnO nanowire gas sensor for detection of benzene and toluene; *Phys. Chem. Chem. Phys.* 15, 17179 **(2013)**.
19. C. P. Gu, S. S. Li, J. R. Huang, C. C. Shi, and J. H. Liu; Preferential growth of long ZnO nanowires and its application in gas sensor; *Sens. Actuat. B* 177, 453 **(2013)**.
20. Y. T. Lim, J. Y. Son, and J. S. Rhee; Vertical ZnO nanorod array as an effective hydrogen gas sensor; *Ceram. Int.* 39, 887 **(2013)**.
21. M. Ghosh, D. Karmakar, S. Basu, S. N. Jha, D. Bhattacharyya, S. C. Gadkari, and S. K. Gupta; Effect of size and aspect ratio on structural parameters and evidence of shape transition in zinc oxide nanostructures; *J. Phys. Chem. Solids* 75, 543 **(2014)**.
22. G. Y. Lu, J. Xu, J. B. Sun, Y. S. Yu, Y. Q. Zhang, and F. M. Liu; UV-enhanced room temperature NO_2 sensor using ZnO nanorods modified with SnO_2 nanoparticles; *Sens. Actuat. B* 162, 82 **(2012)**.
23. S. L. Zhang, J. O. Lim, J. S. Huh, J. S. Noh, and W. Lee; Two-step fabrication of ZnO nanosheets for high-performance VOCs gas sensor; *Curr. Appl. Phys.* 13, S156 **(2013)**.
24. D. Xiang, F. Y. Qu, X. Chen, Z. Yu, L. R. Cui, X. Zhang, J. J. Jiang, and H. M. Lin; Synthesis of porous ZnO nanospheres for gas sensor and photocatalysis; *J. Sol–Gel Sci. Techn.* 69, 370 **(2014)**.
25. C. P. Gu, J. R. Huang, Y. J. Wu, M. H. Zhai, Y. F. Sun, and J. H. Liu; Preparation of porous flower-like ZnO nanostructures and their gas-sensing property; *J. Alloy Compd.* 509, 4499 **(2011)**.
26. M. R. Alenezi, S. J. Henley, N. G. Emerson, and S. R. P. Silva; From 1D and 2D ZnO nanostructures to 3D hierarchical structures with enhanced gas sensing properties; *Nanoscale* 6, 235 **(2014)**.
27. J. Y. Liu, Z. Guo, F. L. Meng, T. Luo, M. Q. Li, and J. H. Liu; Novel porous single-crystalline ZnO nanosheets fabricated by annealing $ZnS(en)_{0.5}$ (en = ethylenediamine) precursor. Application in a gas sensor for indoor air contaminant detection; *Nanotechnology* 20, 125501 **(2009)**.
28. Q. F. Zhai, B. Du, R. Feng, W. Y. Xu, and Q. Wei; A highly sensitive gas sensor based on Pd-doped Fe_3O_4 nanoparticles for volatile organic compounds detection; *Anal. Methods* 6, 886 **(2014)**.
29. Q. Xiang, G. F. Meng, Y. Zhang, J. Q. Xu, P. C. Xu, Q. Y. Pan, and W. J. Yu; Ag nanoparticle embedded-ZnO nanorods synthesized via a photochemical method and its gas-sensing properties; *Sens. Actuat. B* 143, 635 **(2010)**.
30. Q. Simon, D. Barreca, A. Gasparotto, C. Maccato, E. Tondello, C. Sada, E. Comini, A. Devi, and R. A. Fischer; Ag/ZnO nanomaterials as high performance sensors for flammable and toxic gases; *Nanotechnology* 23, 025502 **(2012)**.
31. L. Xu, R. Q. Xing, J. Song, W. Xu, and H. W. Song; ZnO–SnO_2 nanotubes surface engineered by Ag nanoparticles: synthesis, characterization, and highly enhanced HCHO gas sensing properties; *J. Mater. Chem. C* 1, 2174 **(2013)**.
32. G. X. Zhu, Y. J. Liu, H. Xu, Y. Chen, X. P. Shen, and Z. Xu; Photochemical deposition of Ag nanocrystals on hierarchical ZnO microspheres and their enhanced gas-sensing properties; *CrystEngComm.* 14, 719 **(2012)**.
33. F. L. Meng, N. N. Hou, Z. Jin, B. Sun, Z. Guo, L. T. Kong, X. H. Xiao, H. Wu, M. Q. Li, and J. H. Liu; Ag-decorated ultra-thin porous single-crystalline ZnO nanosheets prepared by sunlight induced solvent reduction and their highly sensitive detection of ethanol; *Sens. Actuat. B* 209, 975 **(2015)**.
34. Z. Jin, Y. X. Zhang, F. L. Meng, Y. Jia, T. Luo, X. Y. Yu, J. Wang, J. H. Liu, and X. J. Huang; Facile synthesis of porous single crystalline ZnO nanoplates and their application in photocatalytic reduction of Cr(VI) in the presence of phenol; *J. Hazard. Mater.* 276, 400 **(2014)**.
35. F. L. Meng, H. H. Li, L. T. Kong, J. Y. Liu, Z. Jin, W. Li, Y. Jia, J. H. Liu, and X. J. Huang; Parts per billion-level detection of benzene using SnO_2/graphene nanocomposite composed of sub-6 nm SnO_2 nanoparticles; *Anal. Chim. Acta* 736, 100 **(2012)**.
36. F. L. Meng, Y. Jia, J. Y. Liu, M. Q. Li, Y. F. Sun, J. H. Liu, and X. J. Huang; Nanocomposites of sub-10 nm SnO_2 nanoparticles and MWCNTs for detection of aldrin and DDT; *Anal. Methods* 2, 1710 **(2010)**.
37. N. Barsan and U. Weimar; Conduction model of metal oxide gas sensors; *J. Electroceram.* 7, 143 **(2001)**.
38. J. A. Ragazzo-Sanchez, P. Chalier, and C. Ghommidh; Coupling gas chromatography and electronic nose for dehydration and desalcoholization of alcoholized beverages—Application to off-flavour detection in wine; *Sens. Actuat. B* 106, 253 **(2005)**.
39. D. Kohl, A. Eberheim, and P. Schieberle; Detection mechanisms of smoke compounds on homogenous semiconductor sensor films; *Thin Solid Films* 490, 1 **(2005)**.

Received: 21 September 2015. Revised/Accepted: 25 December 2015.